

1 **Engineered bacteria detect tumor DNA**

2
3 Robert M. Cooper^{1*}, Josephine A. Wright^{2*}, Jia Q. Ng³, Jarrad M. Goyne², Nobumi
4 Suzuki^{2,3}, Young K. Lee³, Mari Ichinose^{2,3}, Georgette Radford³, Feargal Ryan², Shalni
5 Kumar⁴, Elaine M. Thomas³, Laura Vrbanac³, Rob Knight^{5,6,7,8}, Susan L. Woods^{2,3,**}, Daniel
6 L. Worthley^{2,9**} and Jeff Hasty^{1,4,5,8**}.

7
8 1. BioCircuits Institute, University of California, San Diego, La Jolla, CA, USA
9 2. Precision Medicine Theme, South Australia Health and Medical Research Institute,
10 Adelaide, SA, Australia.

11 3. University of Adelaide, Adelaide, SA, Australia
12 4. Department of Bioengineering, University of California, San Diego, La Jolla, CA.
13 5. Molecular Biology Section, Division of Biological Sciences, University of California,
14 San Diego, La Jolla, CA, USA.

15 6. Department of Pediatrics, University of California, San Diego, La Jolla, CA.
16 7. Department of Computer Science & Engineering, University of California, San Diego,
17 La Jolla, CA.

18 8. Center for Microbiome Innovation, University of California, San Diego, La Jolla, CA.
19 9. Colonoscopy Clinic, Brisbane, Qld, Australia.

20 * These authors contributed equally

21 ** Corresponding authors

22
23 **Word count:**

24 Summary paragraph = 209 words

25 The main text (summary paragraph plus body text) = 2500 words

26
27

28 **Summary**

29
30 Advances in bacterial engineering have catalysed the development of living cell
31 diagnostics and therapeutics¹⁻³, including microbes that respond to gut inflammation⁴,
32 intestinal bleeding⁵, pathogens⁶ and hypoxic tumors⁷. Bacteria can access the entire
33 gastrointestinal tract⁸ to produce outputs measured in stool⁴ or urine⁷. Cellular memory,
34 such as bistable switches^{4,9,10} or genomic rearrangements¹¹, allows bacteria to store
35 information over time. However, living biosensors have not yet been engineered to
36 detect specific DNA sequences or mutations from outside the cell. Here, we engineer
37 naturally competent *Acinetobacter baylyi* to detect donor DNA from the genomes of
38 colorectal cancer (CRC) cells, organoids and tumors. We characterize the functionality of
39 the biosensors *in vitro* with co-culture assays and then validate *in vivo* with sensor
40 bacteria delivered to mice harboring colorectal tumors. We observe horizontal gene
41 transfer from the tumor to the sensor bacteria in our mouse model of CRC. The sensor
42 bacteria achieved 100% discrimination between mice with and without CRC. This
43 Cellular Assay of Targeted, CRISPR-discriminated Horizontal gene transfer (CATCH),
44 establishes a framework for biosensing of mutations or organisms within environments
45 that are difficult to sample, among many other potential applications. Furthermore, the
46 platform could be readily expanded to include production and delivery of antibiotic or
47 antineoplastic therapeutic payloads at the detection site.

48
49
50 **Main text**

51
52 Some bacteria are naturally competent for transformation and can sample extracellular
53 DNA directly from their environment¹². Natural competence is one mechanism of
54 horizontal gene transfer (HGT), the exchange of genetic material between organisms
55 outside vertical, “parent to offspring” transmission¹³. HGT is common between
56 microbes¹³ and from microbes into animals and plants¹⁴. Genomic analyses have also
57 found signatures of HGT in the other direction, from eukaryotes to prokaryotes¹⁵, but the
58 forward engineering of bacteria to detect or respond to human DNA via HGT has not
59 been explored. *Acinetobacter baylyi* is a highly competent and well-studied bacterium¹⁶
60 that is largely non-pathogenic in healthy humans¹⁷ and can colonize the murine
61 gastrointestinal tract¹⁸. This combination of traits renders *A. baylyi* an ideal candidate for
62 studying engineered detection of colorectal cancer DNA (Fig. 1). Our CATCH strategy
63 delivers bacterial biosensors to the gastrointestinal tract, where they sample and
64 genetically integrate target tumor DNA. To demonstrate the concept, we use the
65 biosensor to detect engineered tumor cells. We then develop genetic circuits to detect
66 natural, non-engineered tumor DNA sequences, discriminating oncogenic mutations at
67 the single base level. Since the target sequence and output gene are modular, our
68 approach can be generalized to detect arbitrary DNA sequences and respond in a
69 programmable manner, in a range of future contexts.

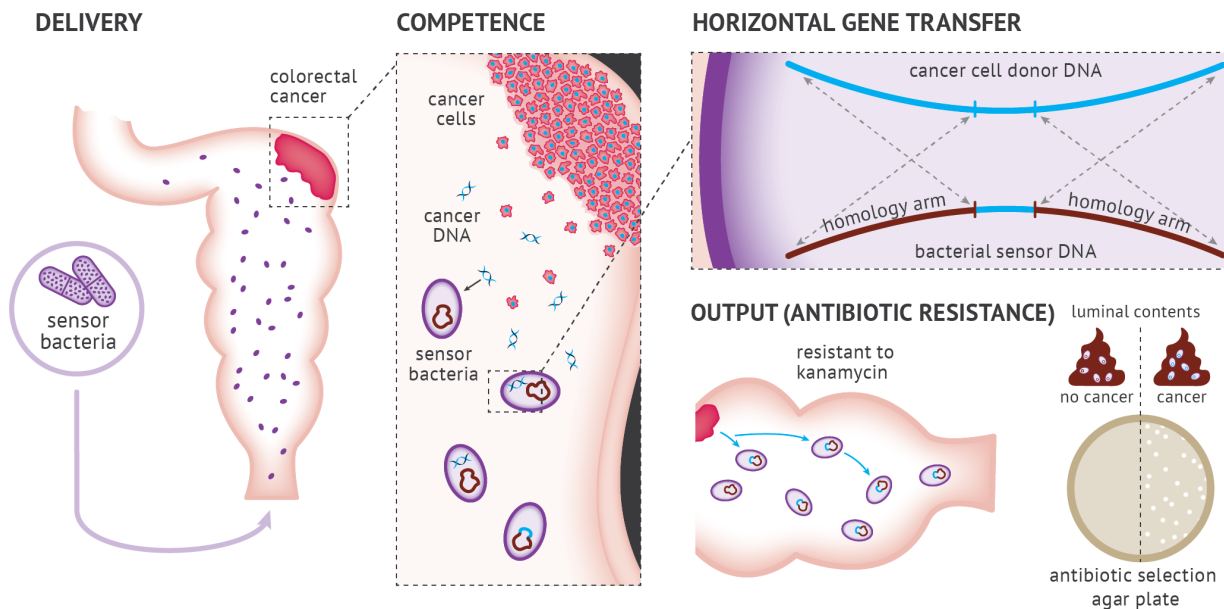


Figure 1. Engineered bacteria to detect tumor DNA. Engineered *A. baylyi* bacteria are delivered rectally in an orthotopic mouse model of CRC. The naturally competent *A. baylyi* take up tumor DNA shed into the colonic lumen. The tumor donor DNA is engineered with a *kan*^R cassette flanked by *KRAS* homology arms (HA). The sensor bacteria are engineered with matching *KRAS* homology arms that promote homologous recombination. Sensor bacteria that undergo HGT from tumor DNA acquire kanamycin resistance and are quantified from luminal contents by serial dilution on antibiotic selection plates.

70

71 Sensor bacteria can detect human cancer DNA

72

73 To test the hypothesis that bacteria could detect human tumor DNA, we generated
74 transgenic donor human cancer cells and sensor bacteria (Fig. 2a). The donor cassette
75 comprised a kanamycin resistance gene and GFP (*kan*^R-GFP) flanked by 1 kb homology
76 arms from human *KRAS* (Fig. 2b-c and Extended Data Fig. 1). *KRAS* is an important
77 oncogene in human cancer, and a driver mutation in *KRAS* often accompanies the
78 progression of simple into advanced colorectal adenomas¹⁹. We stably transduced this
79 donor cassette into both RKO and LS174T human CRC cell lines using a lentiviral vector.
80 To construct the sensor bacteria, we inserted a complementary landing pad with *KRAS*
81 homology arms into a neutral genomic site of *A. baylyi*. We tested both a “large insert”
82 design (2 kb), with a different resistance marker between the *KRAS* arms to be replaced
83 by the donor cassette (Fig. 2b, Extended Data Fig. 2a), and a “small insert” design (8 bp),
84 with the same *kan*^R-GFP cassette as in the tumor donor DNA, but interrupted by 2 stop
85 codons in *kan*^R (Fig. 1 & 2c, Extended Data Fig. 2). The biosensor output was growth on
86 kanamycin plates, measured as colony-forming units (CFUs) after serial dilution.

87

88 We tested both designs using various donor DNA sources, both in liquid culture and on
89 solid agar (Fig. 2a). The “large insert” biosensors detected donor DNA from purified
90 plasmids and genomic DNA both in liquid (Fig. 2d) and on agar (Fig. 2e). On agar, they

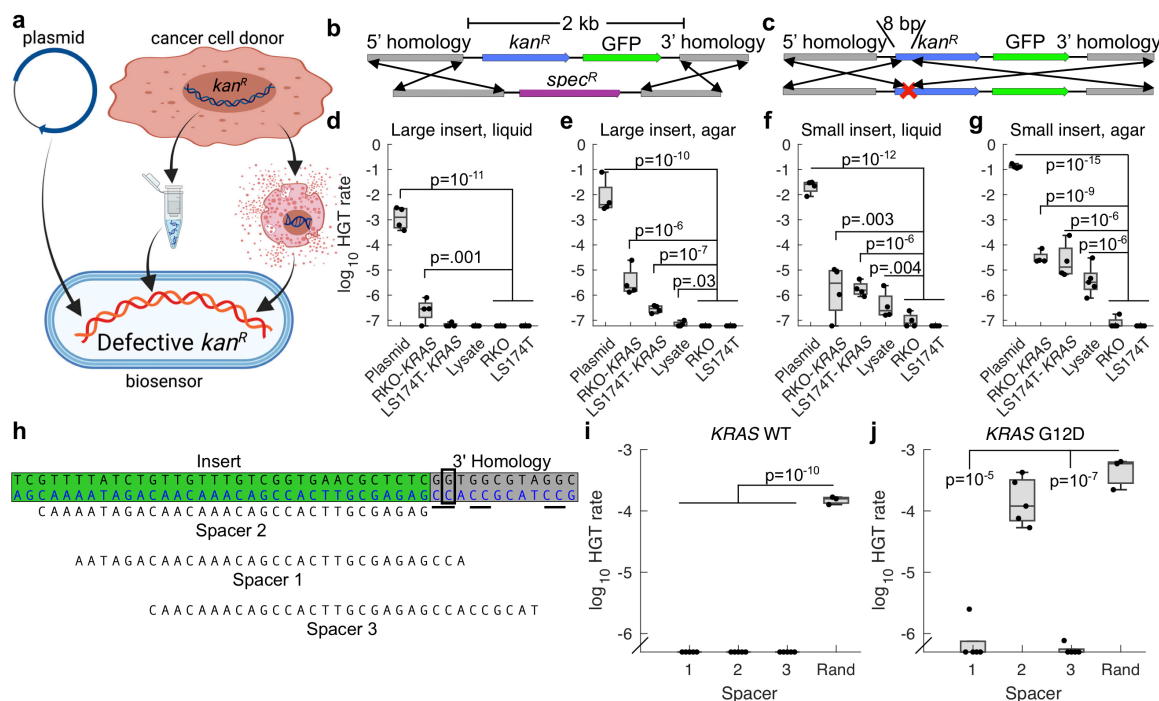


Figure 2: Sensing KRASG12D DNA in vitro. **a-c**, Donor DNA consisting of plasmid, purified cancer cell genomic DNA, or raw lysate (top) recombines into biosensor *A. baylyi* cells (bottom), transferring either a large, 2 kb insert (**b**) or a small, 8 bp insert to repair 2 stop codons (**c**) in both cases conferring kanamycin resistance. **d-g**, *A. baylyi* biosensors were incubated with plasmid DNA, purified RKO-KRAS or LS174T-KRAS genomic DNA, or raw RKO-KRAS lysate, all containing the donor cassette, or purified RKO or LS174T genomic DNA as controls. Biosensor cells included either “large insert” (**b,d,e**) or “small insert” (**c,f,g**) designs, and transformations were performed in liquid culture (**d,f**) or on solid agar surfaces (**e,g**). Two-sample t-tests compared data to combined RKO and LS174T genomic DNA controls for the same conditions. **h**, CRISPR spacers targeting the KRASG12D mutation (boxed), using the underlined PAMs. **i,j**, Fraction of total biosensor cells expressing the indicated CRISPR spacers that were transformed by plasmid donor DNA with wild type (**i**) or mutant G12D (**j**) KRAS. Statistics were obtained using two-sample t-tests. Data points below detection are shown along the x-axis.

also detected raw, unpurified lysate, albeit at just above the limit of detection (Fig. 2e). As expected²⁰, the “small insert” design improved detection efficiency roughly 10-fold, reliably detecting donor plasmid, purified genomic DNA, and raw lysate both in liquid and on agar (Fig. 2f-g, Extended Data Supplemental Movie). Across donor DNA and biosensor design, detection on solid agar was approximately 10-fold more efficient than in liquid culture. Importantly, detection of donor DNA from raw lysate demonstrated that the biosensors do not require *in vitro* DNA purification²¹.

A. baylyi can take up DNA at approximately 60 bp/s²². Given a human genome of 3.2×10^9 bp, each *A. baylyi* cell, including its direct ancestors, can sample roughly 10^{-3} of a human genome in a 24-hour period. Combined with the data shown in Fig. 2g, with a detection rate around 10^{-5} per *A. baylyi* cell for RKO-KRAS and LS174T-KRAS donor DNA, this suggests a detection efficiency of around 1% per processed donor sequence. While this rough calculation assumes a constant DNA processing rate, the result is quite similar to what we found for HGT from *E. coli* to *A. baylyi*²¹.

107 Sensor bacteria can discriminate wild-type from mutant KRAS DNA

108

109 Mutations in codon 12 of *KRAS* are present
110 in 27% of CRC²³, and are common in solid
111 tumors generally²⁴. To test whether sensor
112 bacteria could discriminate between wild-
113 type and mutant *KRAS* (*KRASG12D*),
114 which differ by a single G>A transition, we
115 utilized *A. baylyi*'s endogenous Type I-F
116 CRISPR-Cas system²⁵. We stably
117 transduced an RKO cell line with the *kan*^R-
118 *GFP* donor cassette flanked by wild-type
119 *KRAS* (RKO-*KRAS*), and a second line with
120 *KRASG12D* flanking sequences (RKO-
121 *KRASG12D*). Next, we designed 3 CRISPR
122 spacers targeting the wild-type *KRAS*
123 sequence at the location of the *KRASG12D*
124 mutation, using the *A. baylyi* protospacer-
125 adjacent motif (PAM) of 5'-CC-
126 protospacer-3' (Fig. 2h). We inserted these as single-spacer arrays into a neutral locus in
127 the "large insert" *A. baylyi* sensor genome.
128

129 The sensor bacteria, if effective, should reject wild-type *KRAS* through CRISPR-mediated
130 DNA degradation. Conversely, the *KRASG12D* sequence should alter the target
131 sequence and evade CRISPR-Cas interference. Two of the three spacers blocked
132 transformation by both wild-type and mutant DNA (Fig. 2i-j). However, spacer 2, for
133 which the *KRASG12D* mutation eliminated the PAM site, selectively permitted HGT
134 only with *KRASG12D* donor DNA (Fig. 2i-j). The other common mutations in codon 12
135 of *KRAS* all eliminate this PAM as well²³. Thus, sensor *A. baylyi* can be engineered to
136 detect a mutational hotspot in the *KRAS* gene with single-base specificity.
137

138 Sensor bacteria can integrate cancer DNA in organoid culture

139

140 *Ex vivo* organoid culture faithfully reflects endogenous tumor biology²⁶. We therefore
141 evaluated our sensor and donor constructs in organoid culture (Fig. 3a). We previously
142 used CRISPR/Cas9 genome engineering to generate compound *Braf*^{V600E}; *Tgfr2*^{Δ/Δ};
143 *Rnf43*^{Δ/Δ}; *Znrf3*^{Δ/Δ}; *p16Ink4a*^{Δ/Δ} (BTRZI) mouse organoids that recapitulate serrated CRC
144 when injected into the mouse colon²⁷.

145

146 We transduced BTRZI organoids with the human *KRAS*-flanked donor DNA construct
147 (*KRAS-kan*^R) to generate donor CRC organoids and incubated their lysate with the more
148 efficient "small insert" *A. baylyi* biosensors. As with the CRC cell lines, the sensor *A.*
149 *baylyi* incorporated DNA from donor organoid lysate, but not from control lysates from

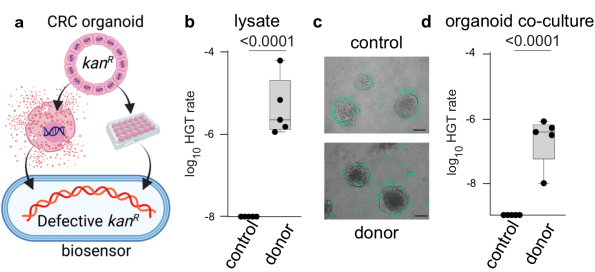


Figure 3: Detection of donor DNA from BTRZI-*KRAS-kan*^R organoids. **a**, Schema depicting *in vitro* co-culture of *A. baylyi* sensor bacteria with BTRZI-*KRAS-kan*^R (CRC donor) organoid lysates or viable organoids to assess HGT repair of kanamycin resistance gene (*kan*^R). **b**, Recombination with DNA from crude lysates enables growth of *A. baylyi* sensor on kanamycin plates with transformation efficiency of 1.4×10^{-5} (limit of detection 10^{-8}). **c**, Representative images of GFP-tagged *A. baylyi* sensor surrounding parental BTRZI (control) and BTRZI-*KRAS-kan*^R donor organoids at 24h. Scale bar 100 μ m. **d**, Co-culture of established CRC BTRZI-*KRAS-kan*^R donor organoids with *A. baylyi* sensor enables growth of *A. baylyi* sensor on kanamycin plates with transformation efficiency of 3.8×10^{-7} (limit of detection 10^{-9}). In **b**, **d**, $n = 5$ independent experiments each with 5 technical replicates, one sample t-test on transformed data was used for statistical analysis with P values as indicated.

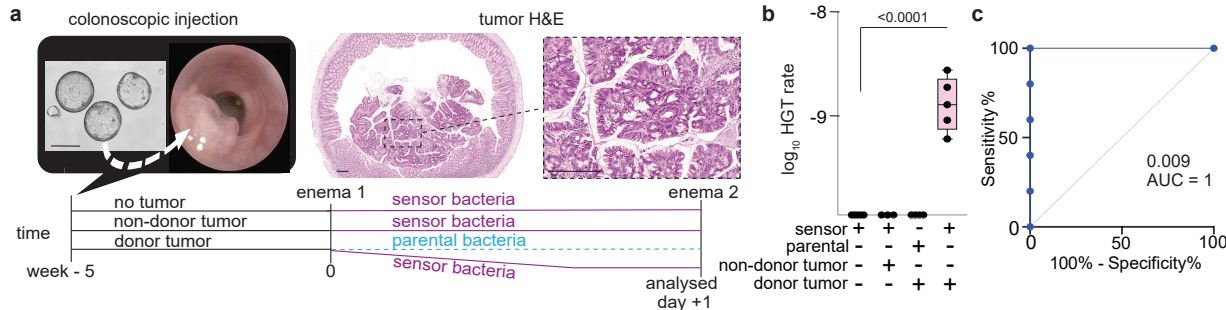


Figure 4. Horizontal gene transfer detected in luminal contents from mice bearing BTRZI-KRAS-kanR tumors after rectal dosing of *A. baylyi* sensor bacteria. a, Schema depicting *in vivo* HGT experiments: generation of BTRZI-KRAS-kanR (CRC donor) tumors in mice via colonoscopic injection of CRC donor organoids with tumor pathology validated by H&E histology, administration of sensor *A. baylyi* or parental *A. baylyi* and analysis of luminal contents. Scale bars 200 μ m. b, rectal delivery of *A. baylyi* sensor to mice bearing CRC donor tumors results in kanamycin resistant *A. baylyi* sensor in luminal contents via HGT with transformation efficiency of 1.5×10^{-9} (limit of detection 1.25×10^{-10}). HGT rate calculated from CFU on Kanamycin/Chloramphenicol/Vancomycin (transformants) and Chloramphenicol/ Vancomycin (total *A. baylyi*) selection plates, n=3-5 mice/group. One-way Anova with Tukey's post-hoc on log₁₀ transformed data was used for statistical analysis with P values shown. c, ROC curve analysis of HGT CFU following enema, AUC=1, p=0.009.

150 the parental organoids (Fig. 3b, Extended Data Fig. 3a). Next, we co-cultured GFP-
151 expressing sensor *A. baylyi* with BTRZI parental or BTRZI-KRAS-kan^R donor organoids
152 for 24 hours on Matrigel. The GFP-expressing sensor bacteria surrounded the organoids
153 (Fig. 3c). Following co-culture with donor, but not parental, organoids, the *A. baylyi*
154 sensor bacteria acquired donor DNA via HGT (Fig. 3d). HGT of kanamycin resistance
155 was confirmed by Sanger sequencing of individual colonies (Extended Data Fig. 3c).
156 Note that these experiments did not test specificity for mutant KRAS, but whether
157 organoid-to-bacteria HGT would occur in organoid co-culture.

158
159 **Sensor bacteria can detect tumor DNA *in vivo***
160

161 Given that cancer-to-bacterial HGT occurred *in vitro*, both in cell lines and in organoid
162 co-culture, we sought to test the CATCH system *in vivo*. We first confirmed that our
163 BTRZI, orthotopic CRC model released tumoral DNA into the fecal stream. In this mouse
164 model of CRC, engineered CRC organoids were injected orthotopically, by mouse
165 colonoscopy, into the mouse colon to form colonic tumors, as previously described²⁷.
166 Using digital droplet PCR, we measured *Braf* mutant tumor DNA in stools collected from
167 tumor-bearing and control mice. The BTRZI model reliably released tumor DNA into the
168 colonic lumen (Extended Data Fig. 4).

169
170 We next conducted an orthotopic CRC experiment (Fig. 4a). NSG mice were injected
171 colonoscopically with donor BTRZI-KRAS-kan^R or non-donor BTRZI organoids or
172 neither. All study groups were housed in separate cages. At week 5, once the tumors had
173 grown into the lumen, 4×10^{10} sensor (or parental) *A. baylyi* bacteria were delivered via
174 rectal enema. 24 hours later, a second enema of sensor or control bacteria were again
175 administered. The mice were subsequently sacrificed and the colorectum harvested with
176 the luminal effluent plated for analysis. Sensor bacteria contained an additional
177 chloramphenicol resistance gene to aid detection, and previous experiments had
178 confirmed that a combination of vancomycin, chloramphenicol and kanamycin provided

179 the best selection for discriminating biosensor HGT from other resistant fecal microbiota.
180 Serial dilutions were plated on agar with different antibiotic combinations for the
181 quantification of HGT in both biosensor and parental *A. baylyi* (Fig 4b).

182
183 Following sensor bacteria delivery, the kanamycin-resistant CFUs were only present in
184 the donor tumor-bearing mice that were administered sensor bacteria. There was no HGT
185 detected in any control groups (Fig. 4b). The resistant colonies were confirmed to be the
186 engineered biosensor strain by antibiotic resistance, green fluorescence, 16S sequencing,
187 and HGT-mediated *kan*^R repair of individual colonies (Extended Data Fig. 5). Our
188 CATCH system perfectly discriminated mice with and without CRC (Fig 4c).
189 Unfortunately, *A. baylyi* biosensors did not establish a sufficient colonising population
190 within the colon to detect tumor bearing mice from collected stool (Extended data Fig. 6).
191 The biosensor population only reached 10⁵ per stool which, based on our *in vitro* studies,
192 is insufficient to detect HGT with the current system (Fig 3d).

193
194 **Sensor bacteria can detect and genotype natural, non-engineered, tumor DNA**
195

196 Finally, we designed living biosensors that can detect and analyze non-engineered DNA
197 without a donor cassette. The *tetR* repressor gene was inserted between the *KRAS*
198 homology arms in the biosensor, and in a second locus, we placed an output gene under
199 control of the P_LtetO-1 promoter²⁸ (Fig. 5a). Here, the output gene was kanamycin
200 resistance for ease of measurement, but the output gene is arbitrary and readily changed.
201 Interestingly, we found that wild type *tetR* is toxic in *A. baylyi*, but we fortuitously
202 isolated a temperature sensitive mutant²⁹ that did not kill the biosensors even at the
203 permissive temperature (see Methods). Clones containing wild type *tetR* could only be
204 isolated in the presence of the inducer anhydrotetracycline (aTc), which inactivates *tetR*,
205 and they could not grow without aTc. We hypothesize that wild type *tetR* disrupts
206 essential gene expression by binding to off-target sites in the *A. baylyi* genome, and that
207 the temperature sensitive mutation also destabilizes binding to off-target sequences, thus
208 increasing binding specificity.

209
210 In this design, expression of the output gene is constitutively repressed (Fig. 5a). Upon
211 recombination with the target DNA, the repressor *tetR* is deleted from the genome and
212 replaced with *KRAS* donor DNA from human cells. If the *KRAS* sequence is wild type at
213 the G12 locus, Cascade, the Type I-F CRISPR-Cas effector complex, detects and degrades
214 it (Fig. 5b). However, if the G12 locus is mutated, the PAM site and therefore CRISPR-
215 Cas targeting are eliminated, and expression from the output gene turns on (Fig. 5c).

216
217 We tested this natural DNA sensor design *in vitro* using PCR products from LS174T and
218 RKO cells as donor DNA. Natural DNA biosensors with a random CRISPR spacer
219 detected DNA sequences from both cell lines (Fig. 5d), and biosensors with the *KRAS*
220 spacer accurately detected only DNA sequence from LS174T cells, which contain the

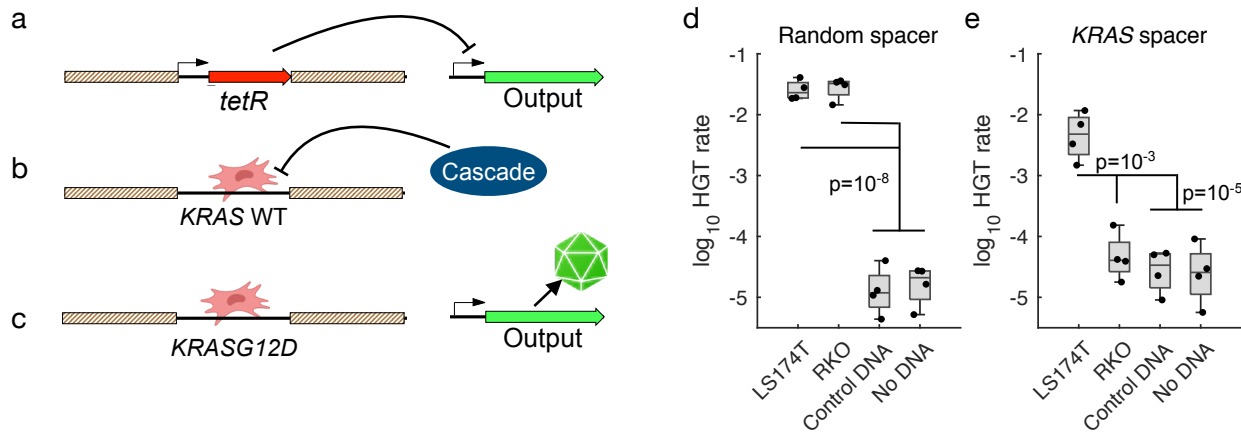


Figure 5: Detection of non-engineered DNA. a, Prior to recombination with target DNA, *tetR* is located between the homology arms on the *A. baylyi* genome and expression of the output gene is repressed. b, Target DNA with the *KRAS* homology arms and wild-type sequence is recognized and degraded by the Type I-F CRISPR-Cas effector complex, Cascade. c, Target DNA with the *KRASG12D* mutation avoids degradation by Cascade, replaces *tetR* in the biosensor genome, and relieves repression of the output gene. d-e, Fraction of biosensors with either a random CRISPR spacer (d) or a spacer targeting wild type *KRAS* (e) that detected donor DNA sequences PCRed from LS174T or RKO cells, unrelated plasmid DNA, or no DNA. Statistics were obtained using 2-sample t-tests.

221 *KRASG12D* mutation, demonstrating biosensor detection and discrimination of natural
222 target DNA.

223

224 Discussion

225

226 In this study, naturally competent *A. baylyi* were engineered to sense donor DNA from
227 cancer cells. Our CATCH biosensor system was optimized *in vitro* and then validated *in*
228 *vivo* using an orthotopic mouse model of CRC. Furthermore, we engineered a CRISPR-
229 based technique to provide specificity for the mutant *KRASG12D* vs. wild-type *KRAS* for
230 both engineered and natural tumor sequences. The sensor bacteria described here
231 demonstrate that a living biosensor can detect tumor DNA shed from CRC *in vivo* in the
232 gut, with no sample preparation or processing. The sensor is highly sensitive and
233 specific, with 100% discrimination between mice with and without CRC. Importantly,
234 engineered donor cassettes are not required for biosensors to detect, discriminate, and
235 report on target sequences, although these natural DNA sensors will need an improved
236 signal-to-background ratio to reliably detect sequences within whole genomic DNA. The
237 homology arms and CRISPR spacers are modular, so this strategy could readily be
238 generalized to detect and analyze arbitrary target sequences of interest.

239

240 *In vitro* DNA analysis helps detect and manage important human diseases, including
241 cancer and infection³⁰. However, *in vitro* sensing requires potentially invasive removal of
242 samples, and many DNA diagnostics cannot achieve clinically relevant sequence
243 resolution, with more advanced techniques remaining too expensive for routine use in
244 all settings³¹. Direct sampling of the gut *in vivo* may offer important advantages. The

245 gastrointestinal tract contains significant DNase activity³², which limits the lifetime of
246 free DNA in both rodents and humans^{18,33,34}, and may thus reduce the information
247 content of downstream fecal samples³⁵⁻³⁷. Bacterial biosensors located *in situ* could
248 capture and preserve DNA shortly after its release, before degradation by local DNases.
249 Perhaps the most exciting aspect of CATCH, however, is that unlike *in vitro* diagnostics,
250 once target DNA is captured, it could be coupled to direct and genotype-complementary
251 delivery of nanobodies, peptides, or other small molecules for the treatment of cancer or
252 infection^{38,39}.

253

254 To realise these opportunities and to translate this technology into the detection and
255 management of human disease, however, the CATCH system will need further
256 development. For *in vivo* applications, biosensors other than *A. baylyi* may be needed that
257 are more compatible with the specific diagnostic niche of interest. Safety and
258 biocontainment would also need to be ensured before use in humans, which could be
259 addressed through *e.g.* genomic recoding to introduce synthetic auxotrophy, which
260 could prevent unwanted HGT and growth^{40,41}. Furthermore, dosing and conditioning
261 regimens are needed to optimise engraftment of biosensors. However, mice are far
262 smaller than humans, and a larger scale would likely benefit *in vivo* CATCH by
263 increasing both the number of biosensors and the released target DNA. Finally, new
264 bioengineering to amplify target DNA through HGT-mediated selection, intercellular
265 quorum sensing circuits, or intracellular genetic memory switches would all help to
266 apply this work^{9,11}.

267

268 CATCH is a new approach for detecting, diagnosing, and in the future potentially
269 treating disease. Furthermore, CATCH may be useful in many non-clinical applications
270 as well, wherever genetic detection is important, continuous surveillance is desirable, or
271 an immediate and localized biologically-generated response would be beneficial.

272 **References**

273

274 1. Slomovic, S., Pardee, K. & Collins, J. J. Synthetic biology devices for in vitro and in
275 vivo diagnostics. *Proc National Acad Sci* 112, 14429–14435 (2015).

276 2. Sedlmayer, F., Aubel, D. & Fussenegger, M. Synthetic gene circuits for the detection,
277 elimination and prevention of disease. *Nat Biomed Eng* 2, 399–415 (2018).

278 3. Lim, W. A. & June, C. H. The Principles of Engineering Immune Cells to Treat Cancer.
279 *Cell* 168, 724–740 (2017).

280 4. Riglar, D. T. *et al.* Engineered bacteria can function in the mammalian gut long-term
281 as live diagnostics of inflammation. *Nat Biotechnol* 35, 653–658 (2017).

282 5. Mark, M. *et al.* An ingestible bacterial-electronic system to monitor gastrointestinal
283 health. *Science* 360, 915 (2018).

284 6. Mao, N., Cubillos-Ruiz, A., Cameron, D. E. & Collins, J. J. Probiotic strains detect and
285 suppress cholera in mice. *Sci Transl Med* 10, eaao2586 (2018).

286 7. Danino, T. *et al.* Programmable probiotics for detection of cancer in urine. *Sci Transl
287 Med* 7, 289ra84-289ra84 (2015).

288 8. Dina, K. *et al.* Effect of Oral Capsule– vs Colonoscopy-Delivered Fecal Microbiota
289 Transplantation on Recurrent Clostridium difficile Infection: A Randomized Clinical
290 Trial. *Jama* 318, 1985–1993 (2017).

291 9. Kotula, J. W. *et al.* Programmable bacteria detect and record an environmental signal
292 in the mammalian gut. *Proc National Acad Sci* 111, 4838–4843 (2014).

293 10. Gardner, T. S., Cantor, C. R. & Collins, J. J. Construction of a genetic toggle switch in
294 *Escherichia coli*. *Nature* 403, 339–342 (2000).

295 11. Courbet, A., Endy, D., Renard, E., Molina, F. & Bonnet, J. Detection of pathological
296 biomarkers in human clinical samples via amplifying genetic switches and logic gates.
297 *Sci Transl Med* 7, 289ra83 (2015).

298 12. Chang, M., Joshua & J, R., Rosemary. Natural competence and the evolution of DNA
299 uptake specificity. *J Bacteriol* 196, 1471–1483 (2014).

300 13. Soucy, S. M., Huang, J. & Gogarten, J. P. Horizontal gene transfer: building the web
301 of life. *Nature Reviews Genetics* 16, 472–482 (2015).

302 14. Robinson, K. M., Sieber, K. B. & Hotopp, J. C. D. A Review of Bacteria-Animal
303 Lateral Gene Transfer May Inform Our Understanding of Diseases like Cancer. *Plos
304 Genet* 9, e1003877 (2013).

305 15. Hotopp, J. C. D. Horizontal gene transfer between bacteria and animals. *Trends Genet*
306 27, 157–163 (2011).

307 16. Young, D. M., Parke, D. & Ornston, L. N. Opportunities for genetic investigation
308 afforded by *Acinetobacter baylyi*, a nutritionally versatile bacterial species that is highly
309 competent for natural transformation. *Annu Rev Microbiol* 59, 519–551 (2005).

310 17. Chen, T.-L. *et al.* *Acinetobacter baylyi* as a Pathogen for Opportunistic Infection ^v. *J
311 Clin Microbiol* 46, 2938–2944 (2008).

312 18. Nordgård, L. *et al.* Lack of detectable DNA uptake by bacterial gut isolates grown in
313 vitro and by *Acinetobacter baylyi* colonizing rodents in vivo. *Environmental Biosafety
314 Research* 6, 149–160 (2007).

315 19. Vogelstein, B. *et al.* Genetic Alterations during Colorectal-Tumor Development. *New
316 Engl J Medicine* 319, 525–532 (1988).

317 20. Simpson, D. J., Dawson, L. F., Fry, J. C., Rogers, H. J. & Day, M. J. Influence of
318 flanking homology and insert size on the transformation frequency of *Acinetobacter
319 baylyi* BD413. *Environmental Biosafety Research* 6, 55–69 (2007).

320 21. Cooper, R. M., Tsimring, L. & Hasty, J. Inter-species population dynamics enhance
321 microbial horizontal gene transfer and spread of antibiotic resistance. *eLife* 6, 8053
322 (2017).

323 22. Palmen, R., Vosman, B., Buijsman, P., Breek, C. K. D. & Hellingwerf, K. J.
324 Physiological characterization of natural transformation in *Acinetobacter calcoaceticus*.
325 *Microbiology+* 139, 295–305 (1993).

326 23. Consortium, T. A. P. G. AACR Project GENIE: Powering Precision Medicine through
327 an International Consortium. *Cancer Discov* 7, 818–831 (2017).

328 24. Priestley, P. *et al.* Pan-cancer whole-genome analyses of metastatic solid tumours.
329 *Nature* 575, 210–216 (2019).

330 25. Cooper, R. M. & Hasty, J. One-Day Construction of Multiplex Arrays to Harness
331 Natural CRISPR-Cas Systems. *AcS Synth Biol* 9, 1129–1137 (2020).

332 26. van de Wetering, M. *et al.* Prospective Derivation of a Living Organoid Biobank of
333 Colorectal Cancer Patients. *Cell* 161, 933–945 (2015).

334 27. Lannagan, T. R. M. *et al.* Genetic editing of colonic organoids provides a molecularly
335 distinct and orthotopic preclinical model of serrated carcinogenesis. *Gut* 68, 684–692
336 (2018).

337 28. Lutz, R. & Bujard, H. Independent and tight regulation of transcriptional units in
338 *Escherichia coli* via the LacR/O, the TetR/O and AraC/I1-I2 regulatory elements.
339 *Nucleic Acids Research* 25, 1203–1210 (1997).

340 29. Pearce, S. C., McWhinnie, R. L. & Nano, F. E. Synthetic temperature-inducible lethal
341 gene circuits in *Escherichia coli*. *Microbiology+* 163, 462–471 (2017).

342 30. Zhong, Y., Xu, F., Wu, J., Schubert, J. & Li, M. M. Application of Next Generation
343 Sequencing in Laboratory Medicine. *Ann Lab Med* 41, 25–43 (2021).

344 31. Iwamoto, M. *et al.* Bacterial enteric infections detected by culture-independent
345 diagnostic tests--FoodNet, United States, 2012-2014. *Mmwr Morbidity Mortal Wkly Rep*
346 64, 252–7 (2015).

347 32. Shimada, O. *et al.* Detection of Deoxyribonuclease I Along the Secretory Pathway in
348 Paneth Cells of Human Small Intestine. *J Histochem Cytochem* 46, 833–840 (1998).

349 33. Wilcks, A., Hoek, A. H. A. M. van, Joosten, R. G., Jacobsen, B. B. L. & Aarts, H. J. M.
350 Persistence of DNA studied in different ex vivo and in vivo rat models simulating the
351 human gut situation. *Food Chem Toxicol* 42, 493–502 (2004).

352 34. Netherwood, T. *et al.* Assessing the survival of transgenic plant DNA in the human
353 gastrointestinal tract. *Nat Biotechnol* 22, 204–209 (2004).

354 35. Imperiale, T. F. *et al.* Multitarget Stool DNA Testing for Colorectal-Cancer Screening.
355 *New England Journal of Medicine* 370, 1287–1297 (2014).

356 36. Zmora, N. *et al.* Personalized Gut Mucosal Colonization Resistance to Empiric
357 Probiotics Is Associated with Unique Host and Microbiome Features. *Cell* 174, 1388–
358 1405.e21 (2018).

359 37. Tang, Q. *et al.* Current Sampling Methods for Gut Microbiota: A Call for More
360 Precise Devices. *Front Cell Infect Mi* 10, 151 (2020).

361 38. Din, M. O. *et al.* Synchronized cycles of bacterial lysis for in vivo delivery. *Nature*
362 536, 81–5 (2016).

363 39. Sepich-Poore, G. D. *et al.* The microbiome and human cancer. *Science* 371, eabc4552
364 (2021).

365 40. Rovner, A. J. *et al.* Recoded organisms engineered to depend on synthetic amino
366 acids. *Nature* 518, 89–93 (2015).

367 41. Mandell, D. J. *et al.* Biocontainment of genetically modified organisms by synthetic
368 protein design. *Nature* (2015) doi:10.1038/nature14121.

369
370

371 **Figure legends**
372

373 **Figure 1. Engineered bacteria to detect tumor DNA.** Engineered *A. baylyi* bacteria are
374 delivered rectally in an orthotopic mouse model of CRC. The naturally competent *A.*
375 *baylyi* take up tumor DNA shed into the colonic lumen. The tumor donor DNA is
376 engineered with a *kan*^R cassette flanked by *KRAS* homology arms (HA). The sensor
377 bacteria are engineered with matching *KRAS* homology arms that promote homologous
378 recombination. Sensor bacteria that undergo HGT from tumor DNA acquire kanamycin
379 resistance and are quantified from luminal contents by serial dilution on antibiotic
380 selection plates.
381

382 **Figure 2: Sensing KRASG12D DNA *in vitro*.** a-c) Donor DNA consisting of plasmid,
383 purified cancer cell genomic DNA, or raw lysate (top) recombines into biosensor *A. baylyi*
384 cells (bottom), transferring either a large, 2 kb insert (b), or a small, 8 bp insert to repair 2
385 stop codons (c), in both cases conferring kanamycin resistance. d-g) *A. baylyi* biosensors
386 were incubated with plasmid DNA, purified RKO-KRAS or LS174T-KRAS genomic DNA,
387 or raw RKO-KRAS lysate, all containing the donor cassette, or purified RKO or LS174T
388 genomic DNA as controls. Biosensor cells included either “large insert” (b,d,e) or “small
389 insert” (c,f,g) designs, and transformations were performed in liquid culture (d,f) or on
390 solid agar surfaces (e,g). Two-sample t-tests compared data to combined RKO and
391 LS174T genomic DNA controls for the same conditions. h) CRISPR spacers targeting the
392 KRAS G12D mutation (boxed), using the underlined PAMs. i,j) Fraction of total biosensor
393 cells expressing the indicated CRISPR spacers that were transformed by plasmid donor
394 DNA with wild type (i) or mutant G12D (j) KRAS. Statistics were obtained using two-
395 sample, one-sided t-tests. Data points below detection are shown along the x-axis, at the
396 limit of detection.
397

398 **Figure 3: Detection of donor DNA from BTRZI-KRAS-kan^R organoids.**
399 Schema depicting *in vitro* co-culture of *A. baylyi* sensor bacteria with BTRZI-KRAS-
400 *kan*^R (CRC donor) organoid lysates or viable organoids to assess HGT repair of
401 kanamycin resistance gene (*kan*^R). b. Recombination with DNA from crude lysates
402 enables growth of *A. baylyi* sensor on kanamycin plates with transformation efficiency of
403 1.4×10^{-5} (limit of detection 10^{-8}). c. Representative images of GFP-tagged *A. baylyi* sensor
404 surrounding parental BTRZI (control) and BTRZI-KRAS-kan^R donor organoids at 24h.
405 Scale bar 100 μ m d. Co-culture of established CRC BTRZI-KRAS-kan^R donor organoids
406 with *A. baylyi* sensor enables growth of *A. baylyi* sensor on kanamycin plates with
407 transformation efficiency 3.8×10^{-7} (limit of detection 10^{-9}). In b, d, n = 5 independent
408 experiments each with 5 technical replicates, one sample t-test on transformed data was
409 used for statistical analysis with P values as indicated.
410

411 **Figure 4. Horizontal gene transfer detected in luminal contents from mice bearing**
412 **BTRZI-KRAS-kanR tumors after rectal dosing of *A. baylyi* sensor bacteria.** a, Schema
413 depicting *in vivo* HGT experiments: generation of BTRZI-KRAS-kanR (CRC donor)
414 tumors
415 in mice via colonoscopic injection of CRC donor organoids with tumor pathology
416 validated
417 by H&E histology, administration of sensor *A. baylyi* or parental *A. baylyi* and analysis of
418 luminal contents. Scale bars 200 μ m. b, rectal delivery of *A. baylyi* sensor to mice bearing

419 CRC donor tumors results in kanamycin resistant *A. baylyi* sensor in luminal contents via
420 HGT with transformation efficiency of 4.75×10^{-9} (limit of detection 1.25×10^{-10}). HGT rate
421 calculated from CFU on Kanamycin/Chloramphenicol/Vancomycin (transformants)
422 and
423 Chloramphenicol/Vancomycin (total *A. baylyi*) selection plates, n=3-5 mice/group.
424 One-way Anova with Tukey's post-hoc on log10 transformed data was used for statistical
425 analysis with P values shown. **c**, ROC curve analysis of HGT CFU following enema, AUC
426 = 1, p = 0.009.
427

428 **Figure 5: Detection of non-engineered DNA.** **a**, Prior to recombination with target DNA,
429 *tetR* is located between the homology arms on the *A. baylyi* genome and expression of the
430 output gene is repressed. **b**, Target DNA with the *KRAS* homology arms and wild-type
431 sequence is recognized and degraded by the Type I-F CRISPR-Cas effector complex,
432 Cascade. **c**, Target DNA with the *KRASG12D* mutation avoids degradation by Cascade,
433 replaces *tetR* in the biosensor genome, and relieves repression of the output gene. **d-e**,
434 Fraction of biosensors with either a random CRISPR spacer (**d**) or a spacer targeting wild
435 type *KRAS* (**e**) that detected donor DNA sequences PCRed from LS174T or RKO cells,
436 unrelated plasmid DNA, or no DNA. Statistics were obtained using 2-sample t-tests.
437

438 **Methods**

439

440 **Data availability**

441 All data generated or analyzed during this study are included in this published article
442 (and its supplementary information files), and raw data files are available upon request.

443

444 **Bacterial cell culture and cloning to generate biosensors**

445 *Acinetobacter baylyi* ADP1 was obtained from the American Type Culture Collection
446 (ATCC #33305) and propagated in standard LB media at 30 or 37 °C. KRAS homology
447 arms were inserted into a neutral genetic locus denoted *Ntrl1*, replacing the gene remnant
448 ACIAD2826. For the “large insert” design, a spectinomycin resistance gene was placed
449 between the KRAS homology arms. For the “small insert” design, two stop codons were
450 placed near the beginning of the *kan*^R gene of the donor cassette, and the broken cassette
451 was inserted into *A. baylyi*. CRISPR arrays were inserted into a neutral locus used
452 previously, replacing ACIAD2186, 2187 and part of 2185. Ectopic CRISPR arrays were
453 driven by a promoter region that included 684 bp from upstream of the first repeat of the
454 endogenous, 90-spacer array.

455

456 For natural DNA biosensors, a temperature-sensitive *tetR* repressor was placed between
457 the KRAS homology arms. An output gene, either *kan*^R or GFP, was placed under control
458 of the P_LtetO-1 promoter in a second neutral locus denoted *Ntrl2*, replacing the gene
459 remnants ACIAD1076-1077. Repeated attempts to clone wild type *tetR* into *A. baylyi*
460 failed, but we fortuitously isolated a temperature sensitive mutant with two mutations:
461 W75R and an additional 8 amino acids on the C terminus. This mutant *tetR* permitted
462 growth at both 30 and 37 °C, but it only repressed its target at 30 °C. The W75R mutant
463 had been isolated previously in an intentional screen. We were able to clone wild-type
464 *tetR* on the inducer aTc, but it was unable grow without aTc at any temperature.

465

466 ***In vitro* biosensor transformation experiments**

467 *A. baylyi* were grown overnight in LB at 30 °C. Cells were then washed, resuspended in
468 an equal volume of fresh LB, and mixed with donor DNA. For transformation in liquid,
469 50 µl cells were mixed with 250 ng donor DNA and incubated in a shaker at 30 °C for 2
470 hours or overnight. For transformation on agar, 2 µl cells were mixed with >50 ng donor
471 DNA, spotted onto LB plates containing 2% wt/vol agar, and incubated at 30 °C
472 overnight. Spots were cut out the next day and resuspended in 500 µl phosphate buffered
473 saline solution (PBS). To count transformants, cells were 10-fold serially diluted 5 times,
474 and 2 µl spots were deposited onto selective (30 ng/ml kanamycin) and non-selective 2%
475 agar plates, with 3 measurement replicates at each dilution level. Larger volumes of
476 undiluted samples were also spread onto agar plates to increase detection sensitivity (25
477 µl for liquid culture, 100 µl for resuspended agar spots). Colonies were counted at the
478 lowest countable dilution level after overnight growth at 30 °C, and measurement
479 replicates were averaged. Raw, unpurified lysate was produced by growing donor RKO
480 cells in a culture dish until confluence, trypsinizing and harvesting cells, pelleting them
481 in a 15 ml tube, resuspending them in 50 µl PBS, and placing the tube in a -20 °C freezer
482 overnight to disrupt cell membranes.

483

484 ***In vitro* statistics**

485 Hypothesis testing was performed using 2-sample, one-sided t-tests in Matlab after
486 taking base 10 logarithms, since serial dilutions produce log-scale data. Where data points

487 were below the limit of detection, they were replaced by the limit of detection as the most
488 conservative way to include them in log-scale analysis. Comparisons between large vs
489 small inserts or liquid vs solid agar culture were performed using paired t-tests, where
490 data were matched for donor DNA and either culture type (liquid vs agar) or insert size,
491 respectively. For Figure 2, d-g) n=4, i,j) n=5 except for random spacer n=3.
492

493 **Creation of RKO and LS174T donor cell lines**

494 To create RKO donor and LS174T donor cell lines, lentiviral expression plasmid pD2119-
495 FLuc2 KRasG12D donor was co-transfected with viral packaging vectors, psPAX2
496 (Addgene; plasmid; 12260) and MD2G (Addgene; plasmid; 12259), into HEK293T cells.
497 At 48 and 72 h after transfection, viral supernatants were harvested, filtered through a
498 0.45- μ m filter, and concentrated using Amicon Ultra Centrifugal Filters (Merck Millipore;
499 UFC910024). Concentrated lentivirus particles were used for transduction. The viral
500 supernatant generated was used to transduce RKO and LS174T cells. 48 hours after
501 transduction, stable transformants were selected with 4 μ g/ml puromycin. Cell lines
502 identity was confirmed by STR analysis. KRAS status of RKO (KRAS wildtype) and
503 LS174T (KRAS G12D) cell lines was confirmed by amplification of a 220bp PCR fragment
504 of the exon 2 KRAS gene, including codons 12 and 13 with primers KRAS F:
505 GGTGGAGTATTGATAGTGTATTAACC and KRAS R:
506 AGAATGGCCTGCACCAGTAA. Sanger sequencing was conducted using the same
507 primers.
508

509 **Creation of BTRZI CRC donor organoids**

510 BTRZI (Braf^{V600E},Tgfbr2^{Δ/Δ},Rnf43^{Δ/Δ} / Znf43^{Δ/Δ};p16 Ink4a^{Δ/Δ}) organoids were generated
511 using CRISPR-Cas9 engineering²⁷ and grown in 50 μ l domes of GFR-Matrigel (Corning; 356231)
512 in organoid media: Advanced Dulbecco's modified Eagle medium/F12 (Gibco; 12634010) supplemented with 1x gentamicin/antimycotic/antibiotic (Gibco; 15710064, 15240062), 10mM HEPES (Gibco; 15630080), 2 mM GlutaMAX (Gibco; 35050061), 1x B27 (Gibco; 12504-044), 1x N2 (Gibco; 17502048), 50 ng/ml mouse recombinant EGF (Peprotech; 315-09), 10 ng/ml human recombinant TGF- β 1 (Peprotech; 100-21).
513 Following each split, organoids were cultured in 10 μ M Y-27632 (MedChemExpress; HY-10583), 3 μ M iPSC (Calbiochem; 420220), 3 μ M GSK-3 inhibitor (XVI, Calbiochem; 361559) for the first 3 days.
514

515 To create BTRZI CRC donor organoids, lentiviral expression plasmid pD2119-FLuc2 KRasG12D donor was co-transfected with viral packaging vectors, psPAX2 (Addgene; plasmid; 12260) and MD2G (Addgene; plasmid; 12259), into HEK293T cells. At 48 and 72 h after transfection, viral supernatants were harvested, filtered through a 0.45- μ m filter, and concentrated using Amicon Ultra Centrifugal Filters (Merck Millipore; UFC910024). Concentrated lentivirus particles were used for transduction. The viral supernatant generated was used to transduce BTRZI organoids by spinoculation. Briefly, organoids were dissociated to single cells using TrypLE. 1x10⁵ single cells were mixed with 250 μ l organoid media; 10 μ M Y-27632; 250 μ l concentrated viral supernatant and 4 μ g/ml polybrene (Sigma; H9268) in a 48 well tray before centrifugation at 600 xg for 90 minutes at 32 °C. Meanwhile, 120 μ l 50:50 ADMEM:Matrigel mixture was added to a cold 24-well tray before centrifugation of this bottom matrigel layer for 40 minutes at 200xg at room temperature, followed by solidifying the Matrigel by incubating at 37 °C for 30 minutes. After spinoculation, cells were scraped from the well and plated on top of the Matrigel monolayer with organoid media. The following day, the media was removed and the

536 upper layer of Matrigel was set over the organoids by adding 120 μ l 50:50
537 ADMEM:Matrigel and allowing to set for 30 minutes before adding organoid media. 48
538 hours after transduction, BTRZI donor organoids were selected with 8 μ g/ml puromycin
539 for 1 week, then maintained in organoid media with 4 μ g/ml puromycin.
540

541 **Organoid lysate mixed with *A. baylyi* sensor bacteria**

542 BTRZI (parental) and BTRZI donor organoids were grown for 5 days in 50 ml Matrigel
543 domes. Organoids were dissociated to single cells with TrypLE, counted and 6×10^5 single
544 cells were collected in PBS and snap frozen. The CFU equivalence of exponentially
545 growing *A. baylyi* sensor culture at OD_{600} 0.35 was ascertained by serial dilution of 3
546 independent cultures with 5 technical replicates plated on 10 μ g/ml Chloramphenicol LB
547 agar plate to be 2.4×10^8 CFU per ml. *A. baylyi* sensor was grown in liquid culture with 10
548 μ g/ml Chloramphenicol to OD_{600} 0.35 before mixing with organoid lysate at a 1:1 ratio
549 and grow overnight on LB agar plates at 30 °C. All bacteria was scraped into 200 μ l
550 LB/20% glycerol before spotting 5x 5 μ l spots onto kanamycin and chloramphenicol
551 plates and grown overnight at 37 °C. Colonies were counted and the dilution factor was
552 accounted for to calculate CFU per ml. Rate of HGT was calculated by dividing the CFU
553 per ml of transformants (Kanamycin plates) by the CFU per ml of total *A. baylyi*
554 (chloramphenicol plates) for 5 independent experiments.
555

556 **Coculture organoids with *A. baylyi* sensor bacteria**

557 For co-culture experiments, 24-well trays were coated with Matrigel monolayers. Briefly,
558 200 μ l 50:50 ADMEM:Matrigel mixture was added to a cold 24-well tray and centrifuged
559 for 40 minutes at 200xg at room temperature, followed by a 30 minute incubation at 37
560 °C to solidify matrigel. BTRZI (parental) and BTRZI donor organoids were dissociated
561 into small clusters using TrypLE and grown for 5 days on a Matrigel monolayer in
562 organoid media without antibiotics before 50 μ l OD_{600} 0.35 *A. baylyi* sensor was added to
563 each well. After 24 hours, organoids were photographed then collected and grown
564 overnight on LB agar plates at 30 °C. All bacteria was scraped into 200 μ l LB/20% glycerol
565 before spotting 5x 5 μ l spots onto kanamycin and chloramphenicol plates and grown
566 overnight at 37 °C. Colonies were counted and the dilution factor was accounted for to
567 calculate CFU per ml. Rate of HGT was calculated by dividing the CFU per ml of
568 transformants (kanamycin plates) by the CFU per ml of total *A. baylyi* (chloramphenicol
569 plates) for 5 independent experiments.
570

571 **Horizontal gene transfer *in vivo***

572 BTRZI donor organoids were isolated from Matrigel and dissociated into small clusters
573 using TrypLE. The cell clusters (equivalent to ~150 organoids per injection) were washed
574 three times with cold PBS containing 10 μ M Y-27632 and then resuspended in 20 μ l 10%
575 GFR matrigel 1:1000 indian ink, 10 μ M Y-27632 in PBS and orthotopically injected into
576 the mucosa of the proximal and distal colon of anaesthetised 10-13 week old NSG mice
577 (150 organoids per injection), as previously described²⁷. Briefly, a customised needle
578 (Hamilton Inc. part number 7803-05, removable needle, 33 gauge, 12 inches long, point 4,
579 12 degree bevel) was used. In each mouse up to 2 injections of 20 μ l were performed. CRC
580 donor tumor growth was monitored by colonoscopy for 5 weeks and the videos were
581 viewed offline using QuickTime Player for analysis. Colonoscopy was performed using
582 a Karl Storz Image 1 Camera System comprised of: Image1 HDTV HUB CCU; Cold Light
583 Fountain LED Nova 150 light source; Full HD Image1 3 Chip H3-Z Camera Head;
584 Hopkins Telescope, 1.9mm, 0 degrees. A sealed luer lock was placed on the working

585 channel of the telescope sheath to ensure minimal air leakage (Coherent Scientific, #
586 14034-40). Tumor growth of the largest tumor visualised was scored as previously
587 described using the Becker Scale (Rex et al, 2012 Am J Gastroenterol). *A. baylyi* sensor was
588 grown in LB liquid culture with 6 μ g/ml Chloramphenicol to OD₆₀₀ 0.6. *A. baylyi* parental
589 was grown in LB liquid culture to OD₆₀₀ 0.6. *A. baylyi* was washed twice with PBS before
590 13 mice received 4x10¹⁰ *A. baylyi* sensor via enema (5 mice without tumors; 3 mice with
591 non-donor BTRZI CRC tumors and 5 mice with BTRZI CRC donor tumors), 4 mice
592 received 4x10¹⁰ *A. baylyi* parental via enema. Enema was performed as per previous
593 publication. Briefly, mice were anaesthetised with isofluorane and colon flushed with 1
594 ml of room temperature sterile PBS to clear the colon cavity of any remaining stool. A
595 P200 pipette tip coated with warm water was then inserted parallel into the lumen to
596 deliver 50 μ l of bacteria into the colon over the course of 30 seconds. After infusion, the
597 anal verge was sealed with Vetbond Tissue Adhesive (3M; 1469SB) to prevent luminal
598 contents from being immediately excreted. Animals were maintained on anaesthesia for
599 5 minutes, and then allowed to recover on heat mat and anal canal inspected 6 hours after
600 the procedure to make sure that the adhesive has been degraded. 24 hours after *A. baylyi*
601 administration, mice received a second enema dosing. Mice were then culled, colons were
602 removed and luminal contents were collected. Luminal contents were grown overnight
603 at 37 °C on LB agar with 10 μ g/ml vancomycin plates. All bacteria was collected into 250
604 μ l LB/20% glycerol, vortexed and stored at -80 °C. 5x 5 μ l serial dilutions were spotted
605 onto LB agar plates containing (1) vancomycin (to detect total *A. baylyi* parental); (2)
606 chloramphenicol; vancomycin (to detect total *A. baylyi* sensor) and (3) kanamycin;
607 chloramphenicol; vancomycin (to detect recombined *A. baylyi* sensor). Colonies were
608 counted and dilutions were factored to calculate CFU *A. baylyi* per mouse. For
609 experiments analysing *A. baylyi* in stool, BTRZI CRC donor tumors were established and
610 monitored as described above. After 5 weeks of tumor growth, 9 mice received *A. baylyi*
611 sensor enemas (5 mice without tumors; 4 mice with BTRZI CRC donor tumors) and 6
612 mice received *A. baylyi* parental enemas (3 mice without tumors and 3 mice with BTRZI
613 CRC donor tumors). Stool was collected 24 hours after *A. baylyi* administration into 250
614 μ l PBS/20% glycerol, vortexed and stored at -80 °C. Stool was analysed on LB agar plates
615 containing (1) vancomycin (to detect total *A. baylyi* parental); (2) chloramphenicol;
616 vancomycin (to detect total *A. baylyi* sensor) and (3) kanamycin; chloramphenicol;
617 vancomycin (to detect recombined *A. baylyi* sensor). Colonies were counted and dilutions
618 were factored to calculate CFU *A. baylyi* per mouse.
619

620 Sequencing gDNA from bacterial colonies grown on kanamycin plates

621 *A. baylyi* transformants were individually picked from kanamycin; vancomycin plates
622 and grown in liquid culture LB supplemented with 25 μ g/ml kanamycin, 10 μ g/ml
623 vancomycin and 6 μ g/ml chloramphenicol. gDNA was extracted using purelink genomic
624 DNA minikit (Invitrogen; K182001). Genomic regions of interest were amplified using
625 Primestar Max DNA polymerase (Takara, # R045A) and primers
626 HGTpcrF: CAAAATCGGCTCCGTCGATACTA;
627 HGTpcrR: TAGCATCACCTTCACCCTC and 16S 27Fa: AGAGTTGATCATGGCTCAG;
628 16S 27Fc: AGAGTTGATCCTGGCTCAG; 16S 1492R: CGGTTACCTTGTACGACTT
629 (16S 27Fa:16S 27Fc: 16S 1492R = 0.5:0.5:1). Sanger sequencing was conducted using the
630 same primers.
631
632

633 **Acknowledgements:** Mr Phil Winning for design assistance with Figure 1. This work was
634 supported by NIH grant R01CA241728. Professor Barbara Leggett and A/Prof. Vicki
635 Whitehall for the original gift of the parental RKO and LS174T human CRC cell lines used
636 in this study.

637
638 **Author contributions:** RC, DW & JH conceived of the concept and study plan. RC, JW,
639 JN, JG, NS, YL, MI, GR, FR, SK, ET, LV, SW, DW, & JH were all involved with data
640 acquisition and or interpretation. RC, JW, RK, SW, DW, & JH were involved in writing
641 and revising the final manuscript.

642
643 **Competing interest declaration:** J.H. is a co-founder and board member with equity in
644 GenCirq Inc, which focuses on cancer therapeutics.

645
646 **Correspondence:** Correspondence and requests for materials should be addressed to:
647 Professor Jeff Hasty: hasty@ucsd.edu
648 Associate Professor Daniel Worthley: dan@colonoscopyclinic.com.au
649 Dr Susan Woods: susan.woods@adelaide.edu.au

650
651 Reprints and permissions information is available at www.nature.com/reprints

652
653 **Extended Data**

654
655 **Extended Data Figure 1:** Plasmid donor DNA used to transfect mammalian cell lines and
656 as positive control donor DNA for *in vitro* experiments.

657
658 **Extended Data Figure 2:** “Large insert (a) and “small insert (b) designs for the
659 biosensors. KRAS homology arms are shown in striped gray with surrounding genomic
660 context outside them. Note that large and small inserts refers to the size of the donor
661 DNA region that must transfer to confer kanamycin resistance, not to the size of the
662 region between homology arms in the biosensor. Two single-base changes introducing
663 nearby stop codons at the beginning of *kan*^R are shown for the small insert design (b).

664
665 **Extended Data Figure 3: Sensor detection of donor DNA from BTRZ1 CRC organoids.**
666 *A. baylyi* sensor bacteria are constitutively chloramphenicol resistant, hence *chlorR* CFUs
667 provide a read-out of total *A. baylyi* present. In contrast, kanamycin resistant sensor
668 bacteria rely on incorporation of donor DNA from CRC organoids to correct the defective
669 *kan* gene and enable growth on kanamycin selection plates. **a** Recombination with lysate
670 from CRC donor organoids enables growth of *A. baylyi* sensor on kanamycin plates.
671 Shown here with representative plates and CFU analysis. **b** After co-culturing
672 established CRC donor organoids with *A. baylyi* sensor, recombination with donor DNA
673 from CRC donor organoids enables growth of *A. baylyi* sensor on kanamycin plates.
674 Shown here with representative images and CFU analysis. Scale bars 200 μ m. **a, b**, Fig 3
675 contains the same data as shown here but presented as HGT rate (kanamycin resistant
676 CFU *A. baylyi* per ml/chloramphenicol CFU *A. baylyi* per ml), n = 5 independent
677 experiments each with 5 technical replicates. **c** Representative Sanger sequencing
678 chromatograms of PCR amplicon covering the region of the *kan* gene containing
679 informative SNPs, to highlight the difference in sequence in gDNA isolated from
680 parental *A. baylyi* sensor bacteria compared to *A. baylyi* colonies isolated from kanamycin
681 plates following mixing with donor organoid lysates or viable organoids.

682

683 **Extended Data Figure 4: High sensitivity digital droplet PCR (ddPCR) detection of**
684 **CRC mutation (*BrafV600E*) in stool DNA isolated from tumour bearing animals (n=3-**
685 **4 mice/group).** a, Representative images of ddPCR data. b, CRC mutation (*BrafV600E*)
686 positive droplets as a % of total droplets. Analysis of no template negative control
687 samples and stool DNA samples from non-tumour bearing animals was used to
688 determine the sensitivity threshold of the assay. Positive control samples contain 10%
689 *BrafV600E* gDNA spiked into stool DNA sample from non-tumour bearing animal. NT,
690 no tumour; Ts, small tumour; Tm, medium tumour; Tl, large tumour; NTC, no template
691 PCR negative control.

692

693 **Extended Data Figure 5:** Horizontal gene transfer is detected in luminal contents from
694 mice bearing BTRZI CRC donor tumors after rectal dosing of *A. baylyi* sensor bacteria. a
695 Recombined *A. baylyi* transformants are GFP positive on
696 kanamycin/chloramphenicol/vancomycin selection plates, scale bar 500 μ m. b
697 Representative Sanger sequencing chromatograms of PCR amplicon covering the region
698 of the kan gene containing informative SNPs to highlight the difference in sequencing
699 DNA isolated from parental *A. baylyi* sensor bacteria compared to *A. baylyi* colonies
700 isolated from kanamycin/chloramphenicol/vancomycin plates in luminal contents from
701 mice bearing BTRZI CRC donor tumors after rectal dosing of *A. baylyi* sensor bacteria

702

703 **Extended data figure 6:** Horizontal gene transfer is not detected in stool from mice
704 bearing BTRZI CRC donor tumors after rectal dosing of *A. baylyi* sensor bacteria. a,
705 Schema depicting *in vivo* HGT experiment: generation of BTRZI-KRAS-kanR (CRC
706 donor) tumors in mice via colonoscopic injection of CRC donor organoids with tumor
707 pathology validated by H&E histology, administration of parental or sensor *A. baylyi*
708 and stool collection. b,c Rectal delivery of *A. baylyi* sensor to mice bearing CRC tumors
709 results in no detection of HGT in *A. baylyi* sensor bacteria present within stool. Data
710 points represent the average CFU per stool from 4 stools per mouse grown on b
711 kanamycin/vancomycin selection plates (*A. baylyi* sensor HGT) or c
712 chloramphenicol/vancomycin selection plates (total *A. baylyi* sensor), n=3-5
713 mice / group. Limit of detection 80 CFUs.

714

715 **Extended Data Movie 1:** *A. baylyi* biosensors taking up plasmid donor DNA.
716 *A. baylyi* were grown overnight, washed into fresh LB, mixed with saturating pLenti-
717 KRAS donor DNA, and sandwiched between an agar pad and a glass bottom dish.
718 Images were taken every 10 minutes. GFP fluorescence indicates that the cells have taken
719 up and genetically integrated the donor DNA cassette.

720

721 **Extended Data DNA Files:**

722 DNA cassettes and surrounding regions corresponding to the “large insert”, “small
723 insert”, and natural DNA sensor designs for *A. baylyi*, and the plasmid donor DNA, as
724 shown in Extended Data 1,2, in Genbank format.